

Numerically exact correlations and sampling in the two-dimensional Ising spin glass

Creighton K. Thomas¹ and A. Alan Middleton²

¹*Dept. of Materials Science and Engineering, Northwestern University, Evanston, Illinois 60208-3108, USA*

²*Department of Physics, Syracuse University, Syracuse, New York 13244, USA*

A powerful existing technique for evaluating statistical mechanical quantities in two-dimensional Ising models is based on constructing a matrix representing the nearest neighbor spin couplings and then evaluating the Pfaffian of the matrix. Utilizing this technique and other more recent developments in evaluating elements of inverse matrices and exact sampling, a method and computer code for studying two-dimensional Ising models is developed. The formulation of this method is convenient and fast for computing the partition function and spin correlations. It is also useful for exact sampling, where configurations are directly generated with probability given by the Boltzmann distribution. These methods apply to Ising model samples with arbitrary nearest-neighbor couplings and can also be applied to general dimer models. Example results of computations are described, including comparisons with analytic results for the ferromagnetic Ising model, and timing information is provided.

I. INTRODUCTION

Just over 50 years ago, Kasteleyn [1] and Fisher and Temperley [2] presented analytic combinatorial methods for counting dimer packings on a lattice; these techniques were soon applied [3, 4] to computing the partition function for the pure ferromagnetic two-dimensional Ising model [5, 6]. These methods continue to be extended and improved to study two-dimensional models in statistical mechanics. Such methods were then extended [7] to numerically compute the thermodynamic properties of disordered magnets. They have allowed for a precise and extensive study of the statistical mechanics of disordered models [8–10]. This paper presents a detailed description of a numerical approach to implement these combinatorial techniques.

To review the power of these techniques in more detail, consider an Ising model where spins on a planar lattice can take on one of two values and the energy is given by the sum over possible ferromagnetic or antiferromagnetic interactions between pairs of neighboring spins. Directly evaluating the partition function of this model with N spins involves a sum of Boltzmann factors over the 2^N spin configurations. But combinatorial techniques allow for a much more compact evaluation. The Ising configurations can be put into correspondence with dimer coverings on a related lattice, where dimer coverings are choices of edges so that each node of the lattice is in exactly one chosen edge. Weighted sums Z_d over all dimer coverings give the partition function Z for the Ising problem, with $Z = Z_d$. The sum over all dimer coverings can in turn be expressed as the Pfaffian [5, 6] of a weighted and signed adjacency-like matrix, the Kasteleyn matrix [1]; for a skew-symmetric matrix, the square of its Pfaffian is equal to its determinant. For the specific case of regular lattices and interactions, the Pfaffians can even be evaluated analytically by direct diagonalization of the Kasteleyn matrix [3, 4], allowing for exact evaluation of thermodynamic quantities and studies of phase transitions. Pfaffians (or also determinants) of $m \times m$ matrices

can be defined directly as the sum over permutations whose number grows exponentially with m , but the matrix can be simplified by column and row eliminations, so that the Pfaffian (or determinant) can be evaluated in time polynomial in m . As the Kasteleyn matrix used here is of size $4N \times 4N$, Z can be found for general planar Ising models in time polynomial in N . (Note that as the arithmetic precision needed for a stable calculation of Z depends on β , there is a β dependent prefactor for the running time which scales roughly as β [11].)

This technique was subsequently generalized to include inhomogeneous couplings between nearest neighboring Ising spins by Saul and Kardar [7] for numerical work. In the Ising spin glass, the nearest neighbor interactions can be either ferromagnetic or antiferromagnetic. For a given random choice of couplings of arbitrary sign, the Pfaffian of the Kasteleyn matrix can be computed and used to derive thermodynamic potentials and susceptibilities. If the couplings are of fixed magnitude J but random sign (the bimodal distribution), the exact dependence of Z on inverse temperature β can be written as a polynomial in $e^{-2\beta J}$ [7]. More generally, this numerical approach has allowed for a detailed study of the thermodynamics of the 2D Ising spin glass, even with continuous disorder distributions. One example of the more important recent developments in these algorithms has been the application of nested dissection and integer arithmetic [8] for computing $Z(T)$ for the bimodal distribution in larger systems. Applying Wilson's dimer sampling technique [12], this numerically exact approach has also been used to generate random samples of configurations of random Ising models [11]. This sampling method bypasses the long equilibration times that arise in Markov Chain Monte Carlo methods.

In this paper, we describe a version of nested dissection as applied to the Pfaffian techniques, with the goal of simplifying and extending the calculation of correlation functions and sample configurations. For a two-dimensional Ising sample with arbitrary nearest-neighbor couplings, we describe how this technique can be used to compute the partition function, to calculate correlation functions,

and to randomly choose sample spin configurations. We find that, due to near cancellations of intermediate sums, multiple precision floating point arithmetic is needed to find accurate results at temperatures of interest for system sizes of size about 20^2 or larger (though the sets of integer fields used in Ref. 8 could also be used for the partition function in the bimodal case). We note that correlation functions were computed at $T = 0$ by Blackman and Poulter for the bimodal case [13] using a different approach. We simplify the sampling technique used in our previous work [11] by simplifying the matrices and by using a different approach to maintain computed correlation functions as spins are sampled. Many of these improvements are based on the FIND (fast inverse using nested dissection) algorithm [14] which computes desired elements of a matrix inverse quickly and was developed to compute nonequilibrium Green's function applications in nanodevices. This particular flavor of hierarchical decomposition is very well suited to the geometry of the mapping between two-dimensional Ising models and dimer coverings. While much of this algorithm is implicit in previous work, we assemble these methods into a form adapted to studying the statistical mechanics of the Ising model, with novel applications to computing correlation functions, and emphasize the nature of the algorithms as a renormalization procedure and clarify the sampling procedure. This formulation is also significantly faster in practice. We present comparisons with analytic results, sample results for the spin glass case, and empirical results for the timings. A version of the computer code for computing partition functions, written in C++, is available in the supplemental materials for this paper at [publisher URL] or by download [15]. Extensions of this version of the code have been checked against analytic predictions for correlation functions in the ferromagnet and against other exact codes for small spin glass samples. This code can be used to study pure, random bond, and spin glass models.

II. ISING MODEL, DIMERS, & PFAFFIAN

In this section, we state the standard Ising spin glass Hamiltonian and recall the mapping between Ising spin configurations and dimer coverings [3, 5, 6, 16]. We also review the definition of the Pfaffian of the Kasteleyn matrix and its relation to the partition function of the Ising model.

A state S of the Ising model in two dimensions on a rectangular sample composed of $L_x \times L_y$ spin variables s_i is given by a choice for each s_i , where each s_i is restricted to $s_i = \pm 1$. The $n = L_x \times L_y$ sites i lie on a square grid. There are 2^n possible spin configurations in the state space \mathcal{S} . The statistical mechanics of this model is governed by the standard Hamiltonian

$$\mathcal{H}(S) = - \sum_{\langle ij \rangle} J_{ij} s_i s_j, \quad (1)$$

where the sample-dependent bond strengths J_{ij} are quenched, i.e., fixed in time, and connect nearest neighbor spin pairs $\langle ij \rangle$. The spins lie on the nodes of a graph G whose edges $\langle ij \rangle$ connect these nearest neighbor pairs. For open or free boundary conditions or for fixed spins on the boundaries, these pairs form the edges of a planar graph. For periodic boundary conditions, nearest neighbor pairs $\langle ij \rangle$ include bonds that wrap the sample around a torus by connecting the top row of the array to the bottom row and the right column to the left column. In equilibrium at temperature $T = \beta^{-1}$, the probability $P(S)$ of a spin state S is $P(S) = \exp^{-\beta \mathcal{H}(S)} / Z$, where the partition function is $Z = \sum_{S \in \mathcal{S}} \exp^{-\beta \mathcal{H}(S)}$. Numerical derivatives of $Z(T)$ with respect to T allow for the computation of energy $E(T)$, the entropy $S(T)$, and the heat capacity $C(T)$. Exact sampling will be taken to mean that configurations S are generated with the correct probability $P(S)$, within numerical accuracy. The correlation functions that will be computed by the algorithm are spin-spin correlation functions, $\langle s_i s_j \rangle$, where the average is taken over all configurations weighted by their equilibrium probability, i.e., $\langle s_i s_j \rangle = \sum_S P(S) s_i s_j$. Computing these correlations allows for a direct measure of the correlation length and the density of relative domain walls. Though we describe the techniques using square lattice samples with open boundaries or with periodic boundaries, the techniques presented generically apply to arbitrary graphs on low-genus surfaces [1, 8].

A given spin configuration S in the Ising model can be represented by a set of relative domain walls and by the value of a single spin. These domain walls can be defined relative to any reference spin configuration S^r ; one simple choice for S^r is the fixed direction configuration S^+ , with all $s_i = +1$. This is the choice that we will use in this paper. (Another example choice would be a ground state configuration S^{gs} that minimizes \mathcal{H} .) The domain walls divide the spins into connected sets of spins that are either all aligned with or all opposite to the spins in S^r . These domain walls can be drawn as loops on the dual graph G_D . The graph G_D has nodes at the center of each (square) plaquette of G . The edges of G_D are dual to the edges in G : they are in one-to-one correspondence, with each edge in G_D crossing one edge in G . Given an arbitrary spin configuration S and a nearest neighbor pair of spins $\langle ij \rangle$, the dual edge that crosses the bond connecting i to j is in a domain wall if $s_i s_j \neq s_i^r s_j^r$. For the choice $S^r = S^+$, the domain walls separate up spins from down spins. As the domain walls are closed loops, an even number of domain wall segments meet at each node in G_D .

The configurations in the Ising model may be put into correspondence with a complete dimer covering problem on a decorated dual graph G_D^* . For the case we are considering, where G is a square grid, each node of G_D can be replaced by a Kasteleyn city [3], which is a subgraph composed of four fully connected nodes. (Note that a Kasteleyn city can be found from a Fisher city [4] by Pfaffian elimination.) By replacing each lattice point in

the dual G_D with a Kasteleyn city, one arrives at the decorated dual graph G_D^* shown in Fig. 1. This larger graph allows for a correspondence between domain walls, equivalent to Ising spin configurations up to a global spin flip $s_i \rightarrow -s_i$, and dimer matchings on G_D^* . For each set of domain walls, there is at least one corresponding dimer covering on the decorated dual lattice G_D^* .

The computation of the partition function Z for the Ising model, a sum over all assignments of Ising spins, can be directly expressed as a related sum over complete coverings of either G^* , the decoration of the graph G by Kasteleyn cities [3], or coverings of G_D^* . For sampling and computing correlation functions, though, it is simpler to start with the decorated dual graph [11, 17]. In a pure Ising model, summing over matchings on G^* corresponds to a high temperature expansion [18], while sums over G_D^* correspond to a low temperature expansion. There is a simple correspondence between domain wall loops in G_D^* and spin configurations: given a set of domain walls, spins are found by setting spins within a single connected region to the same value.

The configurations contributing to the partition function sum correspond to terms in the expansion of the Pfaffian of the Kasteleyn matrix [1]: to describe this correspondence, we first need to define the Kasteleyn matrix and the Pfaffian sum. The Kasteleyn matrix K is a skew-symmetric matrix with non-zero entries for each edge of the decorated graph G_D^* ; the rows and columns of the matrix are indexed by the vertices of the decorated graph. Skew symmetry implies $K_{ab} = -K_{ba}$. A non-zero entry K_{ab} corresponds to an edge in G_D^* connecting vertices a and b . It is a matrix of size $4N \times 4N$. The values of the matrix are ± 1 for edges internal to Kasteleyn cities. Edges that connect cities have weights with absolute value $|K_{ab}| = \exp(-2\beta J_{ij})$, where spins i and j have coupling J_{ij} and the edge ij in G crosses the edge ab in G_D^* . The sign of each K_{ab} is determined by a Pfaffian orientation of the dimer graph (see, e.g., Ref. 6). For the graph G_D^* , a simple Pfaffian orientation is that horizontal edges between Kasteleyn cities are oriented from left to right and vertical intercity edges are oriented from bottom to top, so that if a is to the left of b or b is above a , $K_{ab} > 0$. The orientation of edges internal to a Kasteleyn city can then be set as in Ref. [3] or as described in Sec. 3. Given a proper choice of signs for K_{ab} , the partition function for the original spin problem on a planar graph (without periodic boundaries) can then be shown [1, 5] to be equal to $\text{Pf}(K)$,

$$Z = \sum_S e^{-\beta \mathcal{H}(S)} = \text{Pf}(K), \quad (2)$$

where the Pfaffian of K is defined by a sum over permutations P of node indices,

$$\text{Pf}(K) = \sum_P \epsilon(P) K_{k_1 l_1} K_{k_2 l_2} \cdots K_{k_m l_m}, \quad (3)$$

with $\epsilon(P)$ giving the sign of the permutation $P = (k_1, l_1, \dots, k_m, l_m)$ of the M indices for the nodes of G_D^*

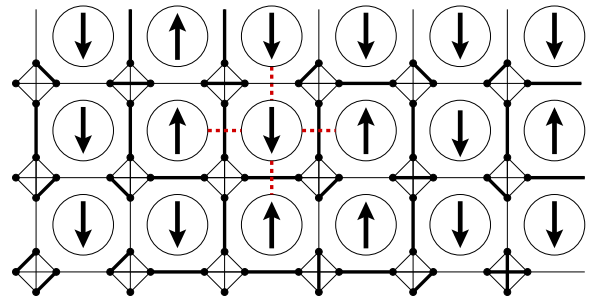


Figure 1: (color online). Correspondence between spin state configurations and complete dimer coverings on the decorated dual graph G_D^* for a periodic spin lattice of size $L_x \times L_y = 6 \times 3$. A sample configuration of Ising spins $s_i = \pm 1$ are represented by the arrows inside the large circles. These spins are coupled by horizontal and vertical bonds of strength J_{ij} . The (red) dashed lines indicate the bonds for one example spin. The spins and bonds are the vertices and edges, respectively, of the Ising model graph G . The nodes of the decorated dual graph G_D^* are drawn as small circles and the edges are indicated by the thin and thick solid lines. The edges of G_D^* are either internal to a Kasteleyn city (the sets of 4 fully connected nodes) or connect neighboring cities. Those that are internal to a city have a weight of 1 while those connecting cities have a weight $w = \exp(-2\beta J_{ij})$, where the J_{ij} is the coupling strength of the bond crossing the dual edge. An example of a complete dimer covering M corresponding to the displayed spin configuration is indicated by the heavy lines: such a choice of edges includes all nodes in G_D^* exactly once. The intercity edges belonging to the covering M separate the up spins from the down spins and so compose the relative domain walls (here we are assuming that the reference configuration S^r is the configuration with all spins up, $s_i = +1$). Note that for any Kasteleyn city surrounded by 4 spins of identical sign, there are 3 ways to arrange the dimers on that city. Two examples of these arrangements can be seen in the lower left and lower right cities. In other cases, the choice of Kasteleyn city edges is uniquely determined by the domain walls.

with $m = M/2 = 2L_x L_y$, and the sum is restricted to the permutations satisfying the orderings $k_1 < k_2 < \dots < k_m$ and $k_1 < l_1, k_2 < l_2, \dots, k_m < l_m$. This choice of signs forces all domain walls relative to a reference configuration to enter with a positive sign; it also leads to the cancellation of terms such that the many-to-one correspondence between dimer coverings and spin configurations becomes one-to-one [19]. The permutation P of indices that enters into the sum represents “matchings” or “dimer coverings”, i.e., choices of edges $e, e_1 = (k_1, l_1), \dots, e_m = (k_m, l_m)$, such that each node in the dual decorated lattice belongs to exactly one edge. For proofs of the correctness of this mapping see, for example, Kasteleyn’s papers [3] and textbook treatments [5, 6]. Note that the partition function for a graph of high genus (e.g., the three-dimensional Ising model) is impractical to compute, as it requires a sum over a number of Pfaffians that is exponential in the genus [8, 16].

The computation of the partition function on planar

graphs is simply given by the evaluation of a single Pfaffian. Computations on a periodic graph are more complicated. Kasteleyn described [1] how to compute the partition functions for dimers on a periodic, i.e., toroidal, lattice. Four Pfaffians are computed for four variations of K , namely K^{++} , K^{-+} , K^{+-} , and K^{--} . We will refer to the set of these four matrices by the notation $K^{\pm\pm} = \{K^{++}, K^{-+}, K^{+-}, K^{--}\}$. For a given choice for $r \in \{+, -\}$ and $s \in \{+, -\}$, the matrix K^{rs} has matrix elements K_{ab} defined according to the standard Pfaffian orientation, except for those elements which have endpoints (a, b) at opposite ends of the square array: these elements correspond to the intercity edges that wrap around the graph, leading to a periodic topology. In the matrix K^{rs} , if an edge connects the a node a in a city that is in column $L_x - 1$ to a node b in column 0, its sign is given by r , while if an edge connects a node in a city in row $L_y - 1$ to a node for a city in row 0, it has sign s . These matrices $K^{\pm\pm}$ can be used to compute the partition functions $Z^{\alpha\beta}$ for $\alpha = \text{P, AP}$ and $\beta = \text{P, AP}$, where P indicates periodic boundary conditions along an axis and AP indicates antiperiodic boundary conditions [negation of the J_{ij} for all horizontal (vertical) edges in a vertical (horizontal) line]. In particular, the partition functions are given by linear combinations

$$Z^{\alpha\beta} = \sum_{(rs) \in (\pm\pm)} L_{rs}^{\alpha\beta} \text{Pf}(K^{rs}) \quad (4)$$

for a 4×4 matrix L [1, 11],

$$L = \frac{1}{2} \begin{pmatrix} 1 & 1 & 1 & 1 \\ -1 & -1 & 1 & 1 \\ -1 & 1 & -1 & 1 \\ -1 & 1 & 1 & -1 \end{pmatrix}. \quad (5)$$

Though the Pfaffian is formally written as a sum over a number of permutations that has a number of terms roughly exponential in N , the Pfaffian of a general $N \times N$ matrix can be evaluated in time polynomial in the number of nodes, in a fashion similar to computing the determinant. However, given the two-dimensional nature of the graph underlying the matrix K , Pfaffians (or determinants) and correlation functions can be computed much more quickly (a lower power of N) than for a general matrix by splitting the set of nodes geometrically in a hierarchical manner [20].

III. CLUSTER MATRICES AND THEIR OPERATIONS

In this section, we first give an introductory outline to the numerical methods we have implemented for rapidly evaluating the partition function and correlation functions. The details are then described in the subsections Sec. III A through Sec. III E. The algorithm for sampling configurations is described in Sec. IV.

The introduction to these methods requires the definition of the intermediate mathematical objects used, the core mathematical steps applied to these objects, and the overall organization of these steps to find the Pfaffian for the whole sample (or ratios of Pfaffians for correlation functions).

The Pfaffian for the whole sample is computed by combining information from smaller regions. We can select a region A on the decorated dual lattice G_D^* by choosing a loop of Ising spins on the spin lattice G : those nodes in G_D^* that are “inside” the loop (generally the smaller set of nodes) will compose the interior set A while those outside the loop compose the exterior, complementary, set \bar{A} . These geometrical regions or clusters have associated matrices and factors. The central mathematical objects used in this procedure are antisymmetric “cluster” matrices $U_A(\mathcal{J})$ and $U_{\bar{A}}(\mathcal{J})$ [14, 20] which depend both on the set of spin couplings $\mathcal{J} = \{J_{ij}\}$ and the region A . The dependence of U on the spin couplings \mathcal{J} that define the given realization of a sample will be implicit in the remainder of this paper and so we will write U_A for $U_A(\mathcal{J})$. A given cluster matrix is indexed by the nodes of the decorated dual lattice that are on the boundary of the clusters: if there are m boundary vertices in the cluster, the matrix U has dimensions $m \times m$. The boundary correlations of dimers (and hence spins on the original graph) are directly related to the cluster matrices U by a matrix inverse. Also associated with each region A is a factor $z(A)$, the “partial Pfaffian”. This factor represents a multiplicative contribution to the overall partition function. It represents a sum over dimer configurations on the interior of A .

The core mathematical steps applied to the cluster matrices are the collection of cluster matrices for neighboring regions into a larger matrix and subsequent elimination (contraction) steps applied to this joint matrix. These elimination steps remove rows and columns from the joint matrix that correspond to nodes that are on the boundary of the original neighboring regions but are not boundary nodes for the union of the two regions. The remaining matrix is then indexed by the boundary nodes of the larger, unified region. This removal of nodes is carried out by Pfaffian elimination, a procedure described in Sec. III A and one that is similar to Gaussian elimination. This directly implements a sum over the the dimer coverings over edges that are shared by the adjacent clusters and incorporates that sum into the partial Pfaffian factor. To collect neighboring regions A , with m_A boundary nodes, and B , with m_B boundary nodes, a square matrix of size $(m_A + m_B) \times (m_A + m_B)$ is filled with the elements of U_A and U_B , in block diagonal form,

$$M_0(W, A, B) = \begin{pmatrix} U_A & W_{ab} \\ -W_{ab}^T & U_B \end{pmatrix}. \quad (6)$$

where the matrix W_{ab} is indexed by the boundary nodes of A and B and has nonzero elements when a and b are the ends of an intercity edge e_{ab} connecting A to B . Partial Pfaffian elimination then removes from the

matrix rows and columns that correspond to the nodes belonging to separating edges in W , while maintaining the overall Pfaffian. The matrix resulting from elimination will be the cluster matrix U_C for the joined regions $C = A \cup B$, with the matrix again indexed by the remaining boundary nodes. The matrix U_C has dimension $m_C = m_A + m_B - 2|W|$. The two steps together, collection and Pfaffian elimination, will be referred to as a “merger”.

The methods for evaluating the partition function $Z = \text{Pf}(K)$ are based on relating the Pfaffian of a region of the sample to the Pfaffians defined for subregions: by recursive application of this relationship, the Pfaffian $\text{Pf}(K)$ of the whole sample can be computed. At the largest scale of this recursion, for example, it turns out that we can write

$$\text{Pf}(K) = \sigma(A^*, B^*) z(A^*) z(B^*) \prod_{e \in W} x_e \quad (7)$$

where the sample is divided geometrically into two regions, A^* and B^* , the $z(A)$ and $z(B)$ factors are “partial Pfaffians” computed recursively. The factors x_e result from the Pfaffian elimination steps described in Sec. III A. The prefactor $\sigma(A^*, B^*) = \pm 1$ is determined by the sign of how the rows and columns of U_{A^*} and U_{B^*} are combined. In turn, we can write, for example,

$$z(A^*) = \sigma(A_1, A_2) z(A_1) z(A_2) \prod_{e \in W_A} x_e \quad (8)$$

where the region A^* is decomposed into regions A_1 and A_2 and W_A is the set of edges that connect these two sets of nodes. Note that the parity factors σ are not strictly needed for computing the partition function in planar graphs, as all that matters in that case is the magnitude of $\text{Pf}(K)$, but they are needed whenever periodic boundary conditions are used. For numerical stability, pivoting operations that permute the rows and columns are used and the choice of pivots may be different for the distinct $K^{\pm\pm}$.

The organization of the cluster matrix mergers is divided into two stages, the up sweep stage and the down sweep stage [14]. In each sweep, matrices representing neighboring or enclosing regions are merged. The organization of these mergers is set by the recursive geometric division of the sample. In the up sweep stage, smaller cluster matrices U_A and U_B for neighboring clusters A and B are merged to create a cluster matrix U_C for the union $C = A \cup B$ of the two clusters. This information sums information over smaller scales into information at larger scales. The up sweep stage is sufficient to compute the partition function of a sample. In the down sweep stage, correlations (and configuration samplings) can be computed. In this stage, the sum of statistical weights of all dimer configurations external to a region is used to find the sum of statistical weights external to smaller regions. If C is the union of clusters A and B , $U_{\bar{C}}$ gives the matrix encoding the sum of statistical weights external to the region C . This matrix is originally found by summing over all dimer configurations external to the

region C . The cluster matrix $U_{\bar{C}}$ can be merged with U_B . This sums over the configuration sums internal to B and the dimer configurations external to both A and B , giving a matrix defined on the boundary of A that represents the sum over dimer configurations external to A , the cluster matrix $U_{\bar{A}}$. At each stage of this recursion, the cluster matrices U_A and $U_{\bar{A}}$ can then be used together to find correlations on the boundary of A . It turns out that the sums of signed mergers of these two matrices gives the spin-spin correlation functions for the Ising spins that lie between A and \bar{A} .

For reference and to provide a flavor of the methods, we present an outline of the steps for computing the partition function and correlation functions; more detailed descriptions of these steps are given in the subsequent subsections:

1. From the bond weights J_{ij} , generate the weights $w_{ij} = e^{-2\beta J}$ for all neighboring spins in the lattice.
2. Generate a binary tree T for the geometric subdivision of the decorated dual lattice G_D^* . Each node of the tree contains geometric information for a region A , the cluster matrices U_A and $U_{\bar{A}}$, and the partial Pfaffian factors $z(A)$. All non-leaf nodes of the tree have pointers to two children representing matrices for two subregions of approximately the same size. The subdivision is terminated at the scale of Kasteleyn cities, which are regions that correspond to the leaves of T .
3. Up sweep: starting from the leaves of T , merge sibling pairs of cluster matrices (U_A, U_B) and factors $z(A)$ and $z(B)$ to compute parent matrices U_C and partial Pfaffian factors $z(C)$.
 - (a) This merging is initiated by collecting the matrices U_A and U_B along with edge weights for the edges W connecting A and B together into a joint matrix $M_0(W, U_A, U_B)$ (see Eq. (6)).
 - (b) Pfaffian elimination then reduces the matrix M_0 into a set of factors x_e and a smaller matrix U_C indexed by the boundary of $A \cup B$.
 - (c) Set $z(C) = \sigma(A, B) z(A) z(B) \prod_{e \in W} x_e$, where $\sigma(A, B) = \pm 1$ gives the total parity of row/column permutations that were used in the rearrangements of M_0 in preparation for Pfaffian elimination and the parity of permutations used for pivoting steps during the Pfaffian elimination.
 - (d) These up sweep steps are carried out recursively, merging clusters up to, but not including, the last pair A^* and B^* representing the initial division of the whole sample.
4. The two largest clusters for A^* and B^* are then merged according to the choice of boundary conditions:

- (a) For open or fixed boundary conditions, simply merge the two top-level cluster matrices U_{A^*} and U_{B^*} . In this case, Pfaffian elimination eliminates all rows and columns and the partition function $\text{Pf}(K)$ is given by Eq. (7).
 - (b) For periodic boundaries, merge the U_{A^*} and U_{B^*} along one of the rows or columns separating them (there are either two rows or two columns separating them for periodic BCs) into a matrix U_{C^*} . Then connect the matrix U_{C^*} with itself along a remaining row to generate two matrices $U_{C^*}^+$ and $U_{C^*}^-$, the former using positive weights for the wrapping edges, the latter using negative weights. Eliminate those connecting edges. Then include wrapping edges along the remaining axis, again using negative and positive edge weights for each of the $U_{C^*}^\pm$. The resulting eliminations give scalars: these overall weights are the Pfaffians $\text{Pf}(K^{\pm\pm})$.
 - (c) Compute $Z^{\text{P,P}}$, $Z^{\text{AP,P}}$, $Z^{\text{P,AP}}$, $Z^{\text{AP,AP}}$ from linear combinations of $\text{Pf}(K^{\pm\pm})$, as given by Eq. (4).
5. Stop here if only the partition function is required. Continue to the next steps to compute correlation functions.
6. Down sweep: descend the tree T , computing cluster matrices for complementary regions and merging interior and exterior matrices to find correlation functions:
- (a) Use the results of the up sweep to initialize the two top level complementary cluster matrices via $U_{\overline{A^*}} = U_{B^*}$ and $U_{\overline{B^*}} = U_{A^*}$.
 - (b) If periodic boundary conditions are used, merge U_{A^*} and $U_{\overline{A^*}}$ and merge U_{B^*} with $U_{\overline{B^*}}$ using the four different choices for wrapping edge weights, i.e., select (r, s) from (\pm, \pm) . Use these mergers to set up four parallel trees for further descent.
 - (c) For all down sweep steps for a planar Ising model or further descending steps in the case of periodic boundary conditions in each of the four trees:
 - i. Given a parent C with known $U_{\overline{C}}$ and children A and B , merge the parent matrix $U_{\overline{C}}$ with U_B to generate matrices $U_{\overline{A}}$ for regions complementary to \overline{A} , as in the FIND algorithm [14].
 - ii. Also merge $U_{\overline{C}}$ with U_A to generate $U_{\overline{B}}$.
 - (d) Compute correlation functions between spins on the corners of any given region A by signed merging of $U_{\overline{A}}$ and U_A . (To find correlation functions for periodic boundary conditions, compute the correlation function as

the weighted sum over four trees as given by Eq. (13).)

A. Pfaffian elimination

Pfaffian elimination simplifies a matrix by setting chosen elements in a row to zero while maintaining the Pfaffian of the matrix as an invariant. This elimination proceeds by a process similar to Gaussian elimination for general matrices, but is applied to skew-symmetric matrices [21]. In Gaussian elimination, the lower triangular elements are set to zero and the determinant is the product of the diagonal elements. In Pfaffian elimination, the diagonal elements of a given skew-symmetric U are zero and Pfaffian elimination aims to set all elements that are more than one step off of the diagonal to zero. The Pfaffian of the matrix is the product of the remaining elements in even-indexed rows (given that the first row has index 0).

Pfaffian elimination can be defined inductively for a skew-symmetric matrix U . Each step simplifies one row to a single non-zero element. Suppose that Pfaffian elimination has been carried out for rows with index less than i , where i is even and the rows are indexed starting with row 0 and that the element in row i and column $i + 1$ is non-zero. Then multiples of row i and column $i + 1$ can be added to rows and columns of higher index to zero out the remaining elements of row i and column i . This addition of rows and columns simplifies the matrix while the Pfaffian is unchanged, in the same fashion as row and column additions in a matrix do not modify its determinant. Specifically, for $j > i + 1$, column $i + 1$ is multiplied by $-U_{i,j}/U_{i,i+1}$ and added to column $j + 1$ and row $i + 1$ is multiplied by the same prefactor and added to row $j + 1$ [21]. Note that the odd rows do not contribute to the Pfaffian when the elimination in the previous even row is completed, so that elimination is applied only to even rows. We use pivoting of the rows and columns that are to be eliminated to improve numerical stability. A pivot is an interchange between indices c and d : the elements of row c are swapped with the elements of row d at the same time columns c and d are swapped. As we use it here, Pfaffian elimination is often carried out only for some subset of rows. Note that rows/columns that are not to be eliminated are not considered for pivoting. The permutations due to pivoting operations place the element with the largest available magnitude in the superdiagonal position, before the elimination is carried out. Each pivot leads to a change of sign in $\text{Pf}(U)$ which is accumulated in the prefactor σ .

Mathematically, Pfaffian elimination carried out for all rows can be used as a factorization scheme, similar to LU factorization via Gaussian elimination [21]. The Pfaffian elimination procedure applies linear operations to U so that $LUL^T = F$ where L is a lower triangular matrix and F is zero except for the superdiagonal elements. The

inverse of a skew-symmetric matrix U is then

$$U^{-1} = L^T F^{-1} L; \quad (9)$$

this procedure of elimination and matrix multiplication is used to find matrix inverses in the sampling of Ising spin configurations (see Sec. IV and Ref. [11]). In the mergings of matrices used here, the rows and columns corresponding to nodes on the boundary of the joined regions are kept, while the rows and columns corresponding to nodes shared by the joined regions are eliminated. The eliminated rows and columns have superdiagonal elements which are multiplied together to give a partial Pfaffian while the rows and columns for the new boundary are carried onto the next stage. Physically, by eliminating rows and columns corresponding to nodes internal to a geometric region, these steps “integrate out” degrees of freedom internal to the new cluster.

B. Geometric dissection

Computations for sparse matrices that are derived from two-dimensional graphs can be very efficiently carried out using the important technique of nested dissection [20]. The row and column indices of the matrix correspond to a numbering of the nodes in a graph. The idea behind nested dissection is to hierarchically subdivide the matrix according to row and column indices that index nodes for distinct compact regions. When subdividing a region into two child regions, the separator for this subdivision can be taken to be either nodes that lie between the two regions or a set of edges that connects the two compact subdivisions. By “compact”, we mean regions of size N whose boundary scales as $O(\sqrt{N})$. The result for the parent region is found by separately computing the results for the two child regions and stitching those two results together using the separator. As a separator can be found with $O(\sqrt{N})$ nodes for a matrix of scale $N \times N$ (i.e., of order L for a spatial region of size $L^2 = N$), with the two subproblems of comparable size, the computation at each scale is for matrices of size $O(\sqrt{N}) \times O(\sqrt{N})$ [20]. The work at each scale is therefore much less than for the dense case where the problem cannot be efficiently subdivided and one needs to consider matrices of size $N \times N$. The first application of nested dissection to efficiently computing spin glass partition functions is described in Ref. [8]. The use of the general concept of nested dissection for sampling dimer configurations was proposed in Ref. [12] and carried out for Ising spin glasses in Ref. [11].

In the form of nested dissection [20] used for dimer sampling [12], a set of nodes in a graph is selected as the separator. This is the form we previously used [11] for sampling Ising spin configurations. Here, we instead use an edge separator with each separating edge having one node in each child region. An example approach that inspired our method is the FIND (fast inverse using nested dissection) technique, which computes some of

the elements of an inverse matrix, as used in computing non-equilibrium Green’s functions in a two-dimensional quantum device. The asymptotic run-time of computing the Pfaffian with either node or edge separators scales with N in the same way, i.e., as $O(N^{3/2})$ but the FIND approach has several advantages for studying the Ising model. These advantages include simplifying the structure of the code as well as allowing for more direct computations of the inverse matrix elements and the Pfaffian ratios used to sample configurations.

In the Ising model, the decorated dual graph G_D^* for an $L_x \times L_y$ square sample with periodic boundaries can be recursively divided by splitting it either horizontally or vertically at each stage into smaller rectangles. Fig. 2 gives an example of this dissection. The geometric dissection of the system into smaller rectangles is described by a binary tree T . Each rectangle is an array of Kasteleyn cities. The leaves of the tree consist of 1×1 arrays, that is, individual Kasteleyn cities, so that the corresponding cluster matrix U_Y for a city Y is a 4×4 matrix. At each stage of the dissection, the graph is divided along the axis with the shortest length and as close to the middle of the rectangle as possible. This division splits the city set by cutting the edges which join neighboring cities; these cut edges comprise the separating set W at each stage. It is important to note that the separator W has a corresponding set of Ising spins: the spins that lie between the two geometric regions and are separated from each other by the edges in the set W (see Fig. 4). The top of the tree T has no boundary and so is associated with a null matrix at the end of the algorithm. However, for efficiency in collecting partial results, the region C^* corresponding to the whole sample has matrices associated with it during intermediate stages of the calculation. The two rectangles A^* and B^* that result from the first division of the sample are the first non-empty regions, with $A^* \cup B^* = C^*$.

This tree structure is used to organize the elimination steps in the FIND-based technique, which consists of two stages: an up sweep which produces the partition function of the system by Pfaffian elimination, and a down sweep which may be used to find inverse matrix elements, bond probabilities, or correlation functions. These stages may be understood as a reorganization to move information about dimer correlations on the region boundaries from one scale to another. First, in the up sweep stage, the cluster matrices, which represent boundary information about couplings that remains after summing over internal degrees of freedom, are joined with cluster matrices in neighboring regions to generate cluster information at a larger scale, for the joint region. This is repeated until the aggregate thermodynamic properties of the entire sample are found. Next, in the down sweep stage, this information may be propagated back down to give correlation results at the smallest scales, and all scales in between. This propagation is effected by merging the correlation information exterior to a region with the interior correlation information.

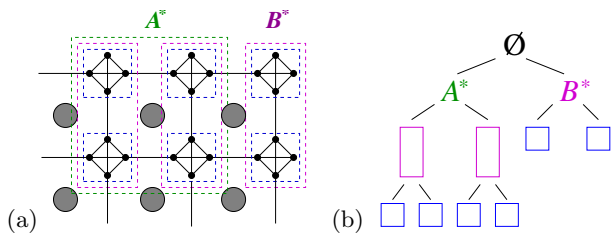


Figure 2: (color online) Depictions of the geometric dissection tree T for an example decorated dual graph. The original Ising system has $L_x \times L_y = 3 \times 2$ spins on a periodic graph; the spins are indicated by gray circles. The decorated dual graph has 3×2 Kasteleyn cities (the sets of four fully connected nodes). At each stage, a parent rectangle of Kasteleyn cities is divided into two roughly equal sibling rectangles, the children. In the algorithms described here, each rectangle A has geometric information, two cluster matrices U_A and $U_{\bar{A}}$, and a partial Pfaffian factor $z(A)$. (a) The nested dissection in real space. The two largest subregions with boundaries, A^* and B^* , indicated. The region C^* in the final stage (not shown for clarity) is the union of A^* and B^* , $C^* = A^* \cup B^*$; at the end of the algorithm, it has no boundary but a matrix corresponding to this region is used as a working matrix when using periodic boundaries. (b) A diagram of the resulting nested dissection tree T . The leaves of the tree are Kasteleyn cities. The root of the tree has no cluster matrix associated with it, as the sample has no boundary, though it has a Pfaffian factor associated with it, which is used to find the partition function for the whole sample.

C. Up sweep stage

The matrix operations for the Pfaffian eliminations carried out in the up sweep stage can be illustrated by an example of the first steps of the algorithm. Describing these first steps allows us to display the matrices used and their correspondence to the graphs showing dimer correlations. Subsequent steps use larger matrices, but have the same structure.

The lowest level steps merge the cluster matrices for two neighboring Kasteleyn cities. Let two such cities be denoted by A and B . These cities each correspond to neighboring nodes on the dual square lattice G_D and are two of the leaves of the tree representing the geometric dissection of G_D^* . The corresponding Kasteleyn matrices, U_A and U_B , are the simplest cluster matrices. The rows and columns of A and B are each indexed by four nodes, so U_A and U_B are each of size 4×4 . In general, due to skew symmetry, only the upper triangular portion of each cluster matrix need be stored in memory. The elements above the diagonal in the matrices U_A and U_B are displayed in Fig. 3(a). Each cluster matrix has a weight associated with it, a partial Pfaffian that accumulates the weights of eliminated rows, which is initialized to be unity, $z(A) = z(B) = 1$. The entries of each matrix have weight of magnitude 1, with signs appropriate for Kasteleyn cities [3]. For the sign conventions and numbering scheme show in Fig. 3(a), all elements of U_A and U_B are positive in the upper triangular section. The edges

joining cities are directed in the positive x and positive y directions, so that the matrix elements K_{kl}^{++} are non-negative for nodes k in cities to the left of or below the city containing node l . Here, the separator W consists of a single edge e joining city A to city B . The weight of this edge is $w = \exp(-2\beta J_{ij})$, where J_{ij} is the bond weight on the connection between spins i and j that is perpendicular to this dual edge e . Note that this edge is not connected to the rest of the lattice and so will be eliminated when merging A and B . To carry out this reduction, the elements of U_A and U_B and the edge weight are copied into a joint temporary matrix $M_0(W, U_A, U_B)$, which is of size 8×8 (28 upper triangular elements). This edge to be eliminated is then placed in the first row of the matrix by permuting the rows of the joint matrix to obtain $M_1(W, U_A, U_B)$. Whenever two rows are interchanged, an overall minus sign is introduced into the Pfaffian factors. In this simple case, only one Pfaffian elimination is applied to $M_1(\{w\}, U_A, U_B)$. This eliminates the connections of the ends of the connecting edge to the rest of the boundaries of A and B , giving a matrix with the first superdiagonal element $x_{1,2}$ is non-zero, but the rest of the first row eliminated. The remaining rows, the third through the last rows, define the new cluster matrix $U_C(W, U_A, U_B)$. This matrix encodes the correlations along the outer boundary of C , the region composed of the two joined cities. This contracted matrix is generally not sparse; see Fig. 3. Using Eq. (8), the partial Pfaffian factor that is stored along with U_C is $z(C) = -z(A)z(B)x$, where the minus sign is included because of the row interchange.

This process of merging adjacent subgraphs of G_D^* , which uses Pfaffian elimination to remove adjacent boundary nodes, is repeated at each scale up to the system size L . Generally, neighboring regions A and B are joined together by copying their entries into a joint matrix M_0 , adding the weights of connections for the set of n edges W that join A to B (W is indicated by jagged lines in Fig. 4), permuting the joint matrix to give M_1 , and then eliminating the first $|W|$ rows. The portion of the matrix that is indexed by the boundary of $C = A \cup B$ is the larger scale cluster matrix U_C . The product of the superdiagonals on the even eliminated rows are used to find $z(C) = \sigma(P)z(A)z(B)\prod_{i=0}^{2(|W|-1)} x_{i,i+1}$, where $\sigma(P)$ is the sign of the permutations carried out in assembling and carrying out pivot eliminations during the elimination and the $x_{i,i+1}$ for even i for the eliminated edges are the superdiagonal elements remaining after Pfaffian elimination. This process is an exact real-space renormalization process on the space of cluster matrices. At each scale, the cluster matrices represent geometric regions whose interactions are computed using their adjacent boundaries, though each of these clusters has many internal degrees of freedom. At the largest length scale, the Pfaffian of the remaining $\mathcal{O}(L) \times \mathcal{O}(L)$ matrix is multiplied by the products $z(A^*)$ and $z(B^*)$ resulting from all lower level mergers to gives the Pfaffian of the entire Kasteleyn matrix, i.e., the partition function $\text{Pf}(K)$.

This procedure of Pfaffian elimination and collection of superdiagonal elements preserves the overall Pfaffian at each stage, since Pfaffian elimination maintains the Pfaffian as an invariant and the Pfaffian of a matrix with only superdiagonal elements in the odd rows is just the product of those superdiagonal elements. The total number of operations in a full up sweep is dominated by the last merger and is of order $\mathcal{O}(N^{3/2})$.

D. Down sweep stage: overview

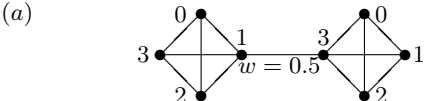
While the up sweep stage can be used to compute a global quantity, e.g., the partition function for given boundary conditions, the subsequent down sweep stage provides a powerful method for computing spatial information such as spin-spin correlation functions. Correlation functions at multiple scales can be computed in a single down sweep, while multiple down sweeps are used to generate sample configurations (see Sec. IV),

The down sweep stage descends the geometry tree T , recursively computing new cluster matrices $U_{\bar{A}}$. These matrices contain information about sums over dimer configurations for the exterior \bar{A} of the geometric regions A . These exterior clusters are merged with the interior cluster matrices that were computed on the up sweep to find spin-spin correlation functions. The computed correlation functions, i.e., the thermal averages $\langle s_i s_j \rangle$, are for pairs of spins i and j that border a geometric cluster A : these spins lie between A and \bar{A} . In our current implementation of the down sweep stage, we compute all pairwise correlations between the four spins that are on the corners of each rectangular region. The results of this computation include correlations between all pairs of neighboring spins, as these are on the corners of the region around a single Kasteleyn city (a 1×1 region).

E. Description of the down sweep stage

The down sweep stage uses as initial data the cluster matrices U_A for each node A of the tree found during the up sweep. As in the FIND method [14], this initial set of cluster matrices is then used to calculate cluster matrices $U_{\bar{A}}$ for the complementary (i.e., exterior) regions \bar{A} . These matrices encode the boundary correlations of dimer matchings resulting from summing matchings over the portion of the sample *surrounding* a geometric region A . This is to be compared with the cluster matrix U_A which contains information about dimer correlations between its boundary nodes resulting from summing all of the dimers within the region A .

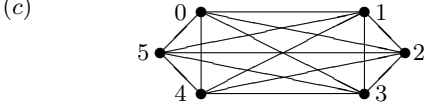
At the highest level, where there are two regions A^* and B^* , $U_{\bar{A}^*} = U_{B^*}$ and $U_{\bar{B}^*} = U_{A^*}$, up to permutations of rows and columns due to differing indexing of the boundary nodes, as A^* is exterior to B^* and B^* is exterior to A^* . The complementary matrix $U_{\bar{A}}$ for a region A at a lower level is computed by merging $U_{\bar{C}}$ with

(a) 

$$U_A = \begin{pmatrix} 1 & 1 & 1 \\ & 1 & 1 \\ & & 1 \end{pmatrix} \quad U_B = \begin{pmatrix} 1 & 1 & 1 \\ & 1 & 1 \\ & & 1 \end{pmatrix}$$

(b)
$$M_0 = \begin{pmatrix} 1 & 1 & 1 & 0 & 0 & 0 & 0 \\ & 1 & 1 & 0 & 0 & 0 & 0.5 \\ & & 1 & 0 & 0 & 0 & 0 \\ & & & 0 & 0 & 0 & 0 \\ & & & & 1 & 1 & 1 \\ & & & & & 1 & 1 \\ & & & & & & 1 \end{pmatrix}$$

$$M_1 = \begin{pmatrix} 0.5 & -1 & 0 & 0 & 0 & 1 & 1 \\ & 0 & -1 & -1 & -1 & 0 & 0 \\ & & 0 & 0 & 0 & 1 & 1 \\ & & & 1 & 1 & 0 & 0 \\ & & & & 1 & 0 & 0 \\ & & & & & 0 & 0 \\ & & & & & & 1 \end{pmatrix}$$

(c) 

$$U_C = \begin{pmatrix} -2 & -2 & -2 & 1 & 1 \\ & 1 & 1 & -2 & -2 \\ & & 1 & -2 & -2 \\ & & & -2 & -2 \\ & & & & 1 \end{pmatrix}; z(C) = 0.5$$

Figure 3: Depiction of merger of Kasteleyn cities A and B connected by an edge of weight $w = \exp(-2\beta J_{ij})$, with w set to 0.5. (a) The rows and columns of the U_A and U_B are indexed by nodes $\{0, 1, 2, 3\}$ and the upper triangular part of these skew-symmetric matrices is shown with the diagonal of zeros omitted. For example, the upper left elements shown in the matrices here are in row 0 and column 1. The signs of the connections correspond to a Pfaffian orientation [3] to consistently count spin configurations. (b) The matrix M_0 is the result of collecting U_A and U_B and the edge weight $w = 0.5$ and is indexed by nodes 0 through 7, with indices from A for the initial part $\{0, 1, 2, 3\}$ and indices from B for the second half $\{4, 5, 6, 7\}$. Permuting rows/columns 0 and 1 and then 1 and 7 gives the matrix M_1 . These permutations place the nodes for the edge to be eliminated in the first two rows of M_1 . (c) After using Pfaffian elimination to remove rows and columns 0 and 1, one is left with a superdiagonal element at $(0, 1)$ of 0.5 (no pivoting is possible in this case) giving a partial Pfaffian $z(C) = 0.5$ and the next generation cluster matrix U_C , indexed by the remaining 6 nodes numbered as shown.

U_B , where C is the parent region for the siblings A and B . The matrices $U_{\bar{C}}$ and U_B are placed into a larger matrix and the edge weights for those edges whose ends are shared by these two boundaries are included. Those edges shared by \bar{C} and B are eliminated by Pfaffian elim-

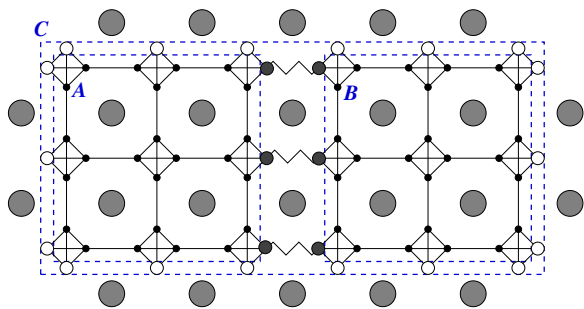


Figure 4: Example of a higher level step of the up sweep stage. The Ising spins on the original lattice whose couplings J_{ij} are relevant to the calculations through this step are indicated by the large grey circles, while the nodes of the decorated dual lattice are indicated by the medium-sized and small circles. The solid straight and jagged lines indicate edges belonging to the decorated dual graph. Two geometric regions on the dual lattice, A and B , each containing 3×3 Kasteleyn cities, are denoted by the (blue) dashed squares. The dual edges W that separate A and B are drawn as jagged lines and join the filled in medium-sized nodes. The small nodes are interior to the regions A and B while the larger nodes (medium-sized open and filled circles) form the borders of A and B . In the up sweep stage (see Sec. III C), given the cluster matrices U_A and U_B for A and B , the separating edges belonging to the separator W are integrated out via Pfaffian elimination, leaving a cluster matrix for C that includes the entire subgraph shown. The cluster matrix U_C is indexed by its border nodes, i.e., the medium-sized open circles connected by the dashed (blue) rectangle.

ination and what remains is the cluster matrix $U_{\bar{A}}$, indexed by the nodes adjacent to A . The entire tree is descended in this fashion, thus generating complementary matrices and correlations between corner spins for each region in the geometry tree T . A step of this process is diagrammed in Fig. 5.

As the $U_{\bar{A}}$ are computed, the clusters U_A and $U_{\bar{A}}$ can be merged via Pfaffian elimination. By comparing the results found using different signs for the connecting edge weights, the spin-spin correlations on the original lattice can be computed. To explain this computation of correlations, we continue to suppose that domain walls are defined using an all spin up reference configuration $S^r = S^+$, so that neighboring Ising spins of opposite sign are separated by a domain wall. Then the Boltzmann weight $e^{-\beta\mathcal{H}(S)}$ of a given spin configuration S is equal to the product $c^r \prod_{e \in X(S)} w_e$ of all weights w_e of edges e that make up the domain wall set $M(S, S^r)$ on the dual graph with $c^r = e^{-\beta\mathcal{H}(S^r)}$, which is a sample and reference state dependent constant. Consider two spins located at i and j in G . In a given spin configuration S , the spins are separated by either an even number or an odd number of domain walls in M . The spins have equal orientations, $s_i = s_j$, if and only if a path in G between the two spins crosses an even number of domain walls. So the correlation function can be found from the average parity of domain walls between the two spins i

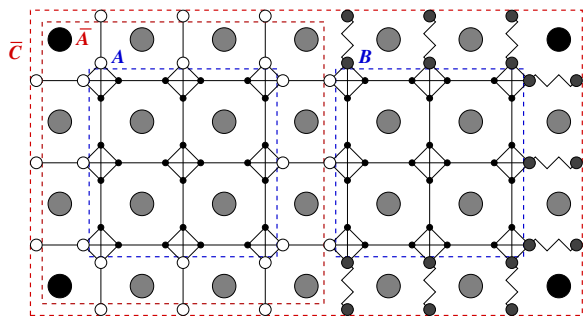


Figure 5: (color online) Diagram of a sample merging of cluster matrices in the down sweep stage for the regions indicated in Fig. 4. The gray and black larger circles indicate the locations of the Ising spins in the original square grid. (The black spins are the corner spins for region C). The matrix $U_{\bar{C}}$ describes the dimer correlations between the nodes that touch the outer (red) dashed line labeled \bar{C} . This matrix sums over correlations external to the spins shown. This cluster matrix $U_{\bar{C}}$ is merged with U_B by eliminating the edges shown by the jagged solid lines. The region B is indicated by the dashed (blue) square on the right of the diagram. The result of the merger is the matrix $U_{\bar{A}}$ describing correlations among the nodes on the boundary of \bar{A} , which is shown by the labeled square (red) dashed line.

and j .

Given a choice of couplings J_{ij} with chosen boundary conditions and temperature, let the equilibrium fraction of spin configurations S with $s_i = s_j$ ($s_i \neq s_j$) be given by $P(s_i = s_j)$ [respectively, $P(s_i \neq s_j)$]. Let $i \rightarrow j$ indicate a path of length ℓ between i and j built up of nearest neighbor pairs $(i, k_1), (k_1, k_2), \dots, (k_{\ell-1}, j)$. For $\ell = 1$, the path is just the single bond (i, j) . The partition function under the constraint that $s_i \neq s_j$ is

$$Z_{s_i \neq s_j} = \sum_{S | s_i \neq s_j} e^{-\beta\mathcal{H}(S)} \quad (10)$$

and can be represented as the restricted sum over matchings M in G_D^*

$$\begin{aligned} & Z_{s_i \neq s_j} \\ &= \sum_{\{M | i \rightarrow j \text{ crosses odd \# edges in } M\}} \epsilon(P) \prod_{e \in M} w(e). \quad (11) \end{aligned}$$

In this formula, the sum over matchings is understood to be restricted to edge choices that obey the restrictions described below Eq. (3) and $\epsilon(P_M)$ is the sign of the permutations in the listing of the nodes in the matching M , so that the many-to-one mapping of dimer coverings to spin configurations is effectively turned into a one-to-one mapping by cancellation of oppositely signed terms. The restriction is to matchings such that the bonds for Ising spin pairs in the path $i \rightarrow j$ are crossed by the dual edges in the matching M an odd number of times. Note that this restriction is independent of the exact path $i \rightarrow j$ and only depends on the endpoints i and

j . A similar correspondence (with the sum over an even number of crossings) holds for expressing $Z_{s_i=s_j}$, with $Z_{s_i=s_j} + Z_{s_i \neq s_j} = Z$.

To compute these restricted partition functions, we compare $\text{Pf}(K)$ with $\text{Pf}(K_{i \rightarrow j})$, where $K_{i \rightarrow j}$ is a modified Kasteleyn matrix. All weights for the edges in G_D^* that cross the chosen path $i \rightarrow j$ contained in G are negated in this modified matrix. That is, the elements of $K_{i \rightarrow j}$ are the same as those in K except where an edge $e \in G_D^*$ is crossed by the path $i \rightarrow j$: in that case, the weight w_e in K is replaced by $-w_e$ in $K_{i \rightarrow j}$. These negations reverse the signs of the weights of matchings M with an odd number of edges of that cross $i \rightarrow j$ while maintaining the sign of matchings with an even number of edges of M crossing that path. To efficiently carry out the computation of $\text{Pf}(K_{i \rightarrow j})$, the path $i \rightarrow j$ is chosen to cross edges that connect a cluster A to its complement \bar{A} . That is the path connect spins that lie between A and \bar{A} . An example showing the negated dual edges is shown in Fig. 6.

These correspondences allow us to write the spin correlation function for a planar Ising model in the form

$$\begin{aligned}
 \langle s_i s_j \rangle &= P(s_i = s_j) - P(s_i \neq s_j) \\
 &= Z^{-1} [Z_{s_i=s_j} - Z_{s_i \neq s_j}] \\
 &= \frac{1}{\text{Pf}(K)} \left[\sum_{\{M|\text{even } i \rightarrow j\}} \epsilon(P_M) \prod_{e \in M} w(e) - \right. \\
 &\quad \left. \sum_{\{M|\text{odd } i \rightarrow j\}} \epsilon(P_M) \prod_{e \in M} w(e) \right] \\
 &= \frac{1}{\text{Pf}(K)} \text{Pf}(K_{i \rightarrow j}) \\
 &= \frac{\text{Pf}[M_0(W_{i \rightarrow j}, U_A, U_{\bar{A}})]}{\text{Pf}[M_0(W, U_A, U_{\bar{A}})]}, \tag{12}
 \end{aligned}$$

The modified list of weights $W_{i \rightarrow j}$ is the set of weights with negated values for all dual edges crossed by the path (any path) from i to j , i.e., $i \rightarrow j$, where again $i \rightarrow j$ lies between A and \bar{A} . Note that $\text{Pf}(K) = \text{Pf}[M_0(W)]z(A)z(\bar{A})$ and $\text{Pf}(K_{i \rightarrow j}) = \text{Pf}[M_0(W_{i \rightarrow j})]z(A)z(\bar{A})$; the cancellation of the common factor $z(A)z(\bar{A})$ gives the last step in the above equation.

This representation of the spin correlations in Eq. (12) defines the procedure for their computation. Correlations between two spins that lie between a region A and its complement $U_{\bar{A}}$ are computed by merging the two matrices U_A and $U_{\bar{A}}$ once using the original weights and again using the modified (partially negated) weights. The ratio of the two resulting Pfaffians gives the spin-spin correlation value. We note that a different approach has been used to compute correlation functions at $T = 0$ [13], where paths between frustrated plaquettes are the basis of the representation in the ground state. For the example shown in Fig. 6, the correlation function is calculated between the two spins diagonally opposite (top left and bottom right) between the outer and inner set of nodes,

whose correlations are given by U_A and $U_{\bar{A}}$. The choice of signs for W could also be modified to compute multispin correlations.

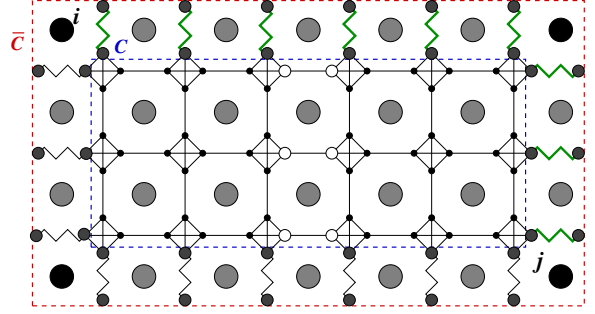


Figure 6: (color online) Diagram of a calculation of a correlation between spins i and j . This calculation uses information computed during the both the up sweep and down sweep stage. The matrices $U_{\bar{C}}$ and U_C are merged using the edge weights on the jagged lines. These edges form the set W . Two mergings are calculated: one for all positive weights for the edges in W and one where the weights are negated for the thicker (green) edges. This gives two Pfaffians for the whole sample. The first Pfaffian has positive contributions from configurations with either an odd or even number of dimer choices (i.e., domain walls) between spins i and j . This is the partition function for the whole sample. The second Pfaffian is the difference between the partition function constrained to have an even number of domain walls between i and j and the partition function constrained to have an odd number of domain walls between i and j .

The calculation of correlations is simplest for planar graphs (Ising models with open or fixed boundary conditions). If periodic boundary conditions are to be used, four different mergers of the two top level matrices U_{A^*} and U_{B^*} are computed. These mergers are computed for all possible pairings of negative or positive weights for bonds that connect the top row to the bottom row of cities or the rightmost column to the leftmost column of cities, as justified in Sec. III C and Ref. [11]. The descent of the tree for each is carried out starting from each of these four choices. There will then be four complementary cluster matrices, $U_A^{\pm, \pm}$, for each geometrical region A . Each complementary cluster matrix will have its own four partial Pfaffian factors $z^{r,s}(\bar{A})$. A spin-spin correlation for periodic boundary conditions (as given by K^{++}) is then the ratio of two weighted sums. The weighted sum in the denominator is the total partition function divided by $z(A)$. The sum in the numerator is the same linear combination of the Pfaffians but with the weights W negated on edges that cross the path $i \rightarrow j$ (i.e., using the weights $W_{i \rightarrow j}$). The partition function for periodic boundary conditions is $Z^{P,P} = \frac{1}{2} \sum_{(r,s)} \text{Pf}(K^{r,s})$. The factor $z(A)$ is common to all terms $\text{Pf}(K) = z(A)z(\bar{A}) \text{Pf}[M_0]$ in the weighted sums and so can be cancelled out. This gives the result that the spin-spin correlation function on a periodic

lattice is the ratio

$$\langle s_i s_j \rangle = \frac{\sum_{(r,s) \in \{(\pm, \pm)\}} \text{Pf}[M_0(W_{i \rightarrow j}, U_A, U_{\bar{A}}^{r,s})] z^{(r,s)}(\bar{A})}{\sum_{(r,s) \in \{(\pm, \pm)\}} \text{Pf}[M_0(W, U_A, U_{\bar{A}}^{r,s})] z^{r,s}(\bar{A})} \quad (13)$$

So the correlation function computations, which require the evaluation of two Pfaffians on a planar graph, require 8 Pfaffians on a torus for each pair of spins. The computation time for the correlation functions for the corner spins on all regions in practice requires about 10 times the amount of computing time as finding only the partition function Z .

IV. SAMPLING

Exact sampling methods select independent configurations according to their probability in the whole sample space. We consider here the problem of generating a sample configuration of a system with probability proportional to the Boltzmann weight $e^{-\beta \mathcal{H}}$. As a contrast with direct sampling, consider Markov chain Monte Carlo (MCMC) methods. In an MCMC method, a sequence of configurations is generated by randomly chosen updates; if the update choices obey detailed balance and can reach all possible configurations, in the limit of large times this sequence will generate sample configurations from the Boltzmann distribution [22]. The number of Monte Carlo updates needed for the approach to fair sampling is often unknown and can be very long. However, MCMC methods can generate exact sampling if coupling from the past [23] can be used to guarantee fair samples (but not necessarily fast mixing times). However, no known coupling methods are practical for Ising spin glass models at low temperatures [24]. Markov chain Monte Carlo methods are of course of great practical use, but the availability of exact sampling in some cases provides for a very useful comparison and the potential for much more rapid calculations for large glassy systems.

The direct sampling methods we use [11] to generate random Ising spin configurations are based on the mapping between dimer and Ising model configurations and on dimer sampling methods [12] that use nested dissection. By directly selecting a random matching on the decorated dual graph G_D^* with the proper probability, we fairly select a set of relative domain walls and hence the relative orientations of the spins on the original lattice. We report here on a modification of the method used in Ref. [11]; here we use the edge separators W [14] described in Sec. III rather than a node separator [12]. This modification significantly speeds up the sampling algorithm for the Ising model, as the dimension of the matrices to be factorized are reduced by a factor of three from those used in Ref. 11. The implementation of the algorithm is also simplified.

As in the computation of the partition function and correlation functions, the direct sampling calculations rely on a geometric dissection. The tree used for sampling

differs some from that described in Sec. III for computing partition functions and correlation functions. For sampling configurations with periodic boundary conditions, we start this modified dissection with a cluster C^* which is formed by joining the two system halves A^* and B^* along a single line of spins. The cluster C^* includes all of the nodes in the decorated dual graph G_D^* , but does not include the edges at the top or right that connect the top row of nodes to the bottom row or the right column to the left column. These edges that are left out are those used to complete the periodic boundary conditions. See Fig. 7(a) for a drawing of C^* and the initial separator. All of the edges internal to the region C^* are contracted out by Pfaffian elimination in an up sweep to give the cluster matrix U_{C^*} . This matrix $M(C^*)$ is used in the first stage of spin assignment. In this first stage, the Ising spins that form the bottom row of the sample are chosen. As the probability distribution is symmetric with respect to global spin reversals, we can simply fix an initial spin, the spin at the lower left, to have the value +1. The orientation of the remaining spins that lie along the bottom row of C^* are then assigned sequentially first along the bottom row. The spins along the left column are then assigned. This assignment is based on the probabilities of domain walls separating neighboring spins in the bordering row and column. These probabilities are found by effectively computing the correlation functions between spins in the lower row and left column. Note that, in principle, any order of spin assignment for these outer border spins could be used. It is possible that numerical stability might be improved by choosing an alternate order of spin assignments; we chose the nearest neighbor sequence for simplicity.

Once all spins around the boundary of the sample are fixed, the process becomes simpler. Spin assignments are decided at finer scales by descending the tree recursively. In each subsequent step, the spins surrounding a region C have been fixed by prior assignment. The probabilities of domain wall sections crossing between the spins lying between two child regions A and B are computed. The spins between the two child regions A and B are then assigned by using these probabilities of relative domain walls. As the assignments are made, the probabilities for remaining parts of the separator are updated. These newly assigned spins then form the boundaries for the child regions of A and of B . These steps are shown for a sample spin assignment in Fig. 7.

The iterative assignment of spins along the separators uses the inverse of a cluster matrix to compute correlation functions. The spins are randomly chosen according to these correlation functions. An essential part of this approach is that when a spin is fixed by such a choice, the inverse of the cluster matrix can be updated efficiently and incrementally [12, 25]. This incremental update makes the sampling procedure running time for selecting a single spin configuration proportional to the time of computing the partition function (though with a larger prefactor). A summary outline of the procedure is

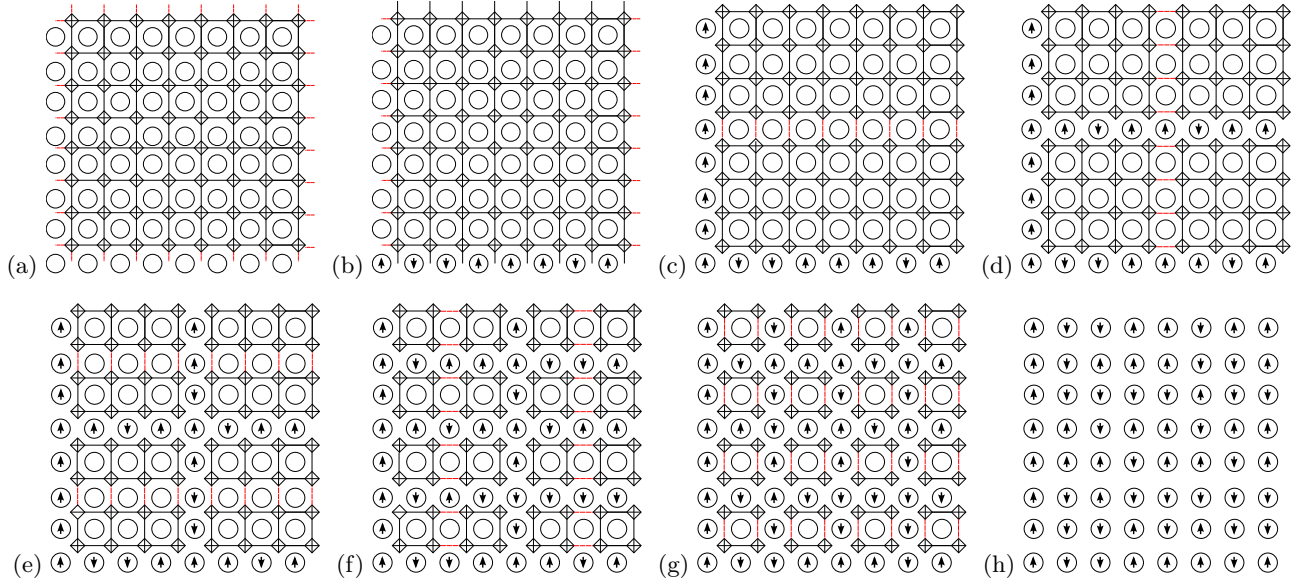


Figure 7: (color online) Steps for exact sampling on a periodic Ising spin lattice of size $L_x \times L_y = 8 \times 8$. Empty circles indicate unknown spins. Arrows indicate assigned spins: \uparrow for $s = +1$ and \downarrow for $s_i = -1$. Separators W are drawn as dashed light (red) lines. The regions of the graph G_D^* used at each stage are shown by solid darker lines. (a) The first region C^* is shown. The separator W (these wrapping edges are drawn as separated half edges) connects C^* to itself. Given a seed spin, deciding which edges in W are in the matching M along the bottom row fixes the spins for step (b). (b) The spins decided in (a) fill the lowest row. The remaining separator along the column is to be filled in for the start of the next step. (c) In all subsequent steps, including this step, the boundary conditions are fixed. The region C^* is separated into the lower half A^* and the upper region B^* . Choices are made for the dual edges connecting A^* to B^* . (d) Three edges are chosen for each of the two separators to fix the 3 spins for each region pair. (e) Four separators are used to set 12 spins. (f) Eight separators are used to set eight spins. (g) In this final stage, there are 16 separators. One edge choice is made for each, fixing the remaining undecided spins. (h) The final spin assignment.

presented in Sec. IV C; the next sections Sec. IV A and Sec. IV B give more details of the algorithm.

A. Computing domain wall probabilities

Given two regions A and B and their edge separator W , the domain wall probabilities are calculated using the inverse of K_W , the Kasteleyn matrix that incorporates the effects of both the values of the boundary spins surrounding $A \cup B$ and the weights on the edges in W . Note that boundary spins around the region $A \cup B$ are taken to be fixed, except at the highest level. These fixed spins affect the weights of the intercity edges at the boundaries of A and B . These weights are computed for a reference configuration where the spins at the boundary of A and B are fixed to the values decided at the higher levels of the tree. We can continue to use all spins set to $s_i = +1$ for the spins interior to A and B . It follows that if a spin j neighbor to i in the region A is fixed to be $s_j = -1$, the weight $w(e)$ for the edge e crossing the bond $\langle ij \rangle$ is set to be $\exp(2\beta J_{ij})$. If the boundary spin is fixed to $s_j = +1$, then the usual weight is used, $w(e) = \exp(-2\beta J_{ij})$. At each stage of the spin assignment, then, we recompute the matrices U_A and U_B using these weights that depend on the boundary spins for $A \cup B$. The matrix K_W is found by collecting U_A and U_B into a single matrix and then linking the matrices using the edge weights that connect A and B . Matrix inversion using Pfaffian factorization is then used to compute the matrix K_W^{-1} .

The inverse matrix K_W^{-1} allows for the simple calculation the probability of any given separating edge being part of a domain wall. These calculations Eqns. (16,17) use the Pfaffian analog of the Jacobi determinant identity, which states that

$$\frac{\text{Pf}(U_{k,l})}{\text{Pf}(U)} = \pm \text{Pf}(\{U^{-1}\}_{k,l}), \quad (14)$$

where $U_{k,l}$ is the matrix with rows and columns k and l removed. The notation $\{U^{-1}\}_{k,l}$ indicates the 2×2 submatrix of U^{-1} which is built out of the intersections of rows and columns k and l , i.e.,

$$\{U^{-1}\}_{k,l} = \begin{pmatrix} 0 & U_{k,l}^{-1} \\ -U_{k,l}^{-1} & 0 \end{pmatrix}, \quad (15)$$

where $k < l$, so that $\text{Pf}(\{U^{-1}\}_{k,l}) = U_{k,l}^{-1}$. Since the ratio of Pfaffians of Kasteleyn matrices $\text{Pf}(K)$ is the ratio of partition functions Z , probabilities can be computed using the identity Eq. (14). Let the edge on the decorated dual graph that separate the neighboring spins i and j have nodes a and b . The probability of including an edge e_{ab} as part of a domain wall that separates the two spins is then given by the expression

$$P(e_{ab} \in M) = |[K_W]_{ab}[K_W^{-1}]_{ab}|. \quad (16)$$

The result Eq. (16) then follows from the probability being the product of the weight of the chosen edge and the

weight of dimer configurations that don't include nodes k and l (i.e., $\text{Pf}(K_W)_{k,l}$) divided by the total weight $\text{Pf}(K_W)$. When W is the separator for regions A and B with fixed boundary spins, the ab element of K_W is given by $[K_W]_{ab} = w_{ab}$. The situation is different for the top level matrix C^* , where W "separates" $C^* = A^* \cup B^*$ from itself, i.e., the edges connect boundary nodes on C^* to each other. In this case, $[K_W]_{ab} = w_{ab} + [U_{C^*}]_{ab}$. In addition, the probability for selecting an edge that connects C^* to itself is given by a weighted sum over the four possible boundary dimer orientations,

$$P(e_{ab} \in M) = \left| \frac{\sum_{(r,s)} w_{ab}^{r,s} \text{Pf}(K_W^{(r,s)}) [K^{(r,s)}]_{ab}^{-1}}{\sum_{(r,s)} \text{Pf}(K_W^{r,s})} \right| \quad (17)$$

The equation for domain wall probabilities at the highest level in the periodic lattice follows from Eq. (5) and Eq. (14) and cancellations of common factors similar to those that led to the result Eq. (12).

Once the probability of choosing an edge is computed, a random number y is chosen in the interval $[0, 1)$ to decide whether to accept the addition of edge e_{ij} to M . If $y < P(e_{ij} \in M)$ the edge e is included in the sampled matching, otherwise it is excluded. Given the resulting choice, the matrix K_W^{-1} is then updated by the method described in Sec. IV B. We note here the contrast with methods for dimer covering sampling that are based on node separators [11, 12]. In these methods, a chosen node that is between regions A and B was matched. The probabilities computed were the probability of choosing each edge that matched the chosen node, with the sum of these probabilities being unity. From the Jacobi identity, the conditional probabilities for these forced node matching could be found without recomputing all of the elements of K^{-1} ; these probabilities are given by the Pfaffian of a submatrix that grows with the number of fixed nodes [12]. Here, instead, nodes on the boundary may or may not be matched, depending on whether an edge is chosen or not, so the same approach cannot be used. Instead, inspired by the approach of Ref. [25], we update the inverse matrix using the Sherman-Morrison formula. Note that only $|W| - 1$ edges are need be chosen for each separator W , as the last choice of an edge is forced by consistency in the spin assignments (or, equivalently, parity in the dimer covering.)

B. Updating K^{-1} using the Sherman-Morrison formula

After the assignment of one spin value, the choice of whether the corresponding edge is included in the matching is fixed for the remainder of the calculation; all subsequent bond probabilities along the separator W must be computed conditioned upon this choice. This is accomplished by modifying the inverse Kasteleyn matrix K_W^{-1} for the edge separator. The Sherman-Morrison formula [25] allows for quickly recomputing the inverse of a

matrix when modifications of the original matrix are confined to one (or a small number) of rows and columns. Here, we apply this formula to set specific edges of K_W to zero. One formulation of the Sherman-Morrison formula is that for any matrix A , and row vectors u and v ,

$$(A + uv^T)^{-1} = \left(A^{-1} - \frac{A^{-1}uv^T A^{-1}}{1 + v^T A^{-1}u} \right). \quad (18)$$

In the sampling algorithm, the choice of whether to force the inclusion of an edge or exclude it from M modifies the skew-symmetric matrix K_W in two rows and columns at the same time. When including an edge e_{ab} , all elements of K_W in rows and columns a and b are set to zero, except the elements $[K_W]_{a,b}$ and $[K_W]_{b,a}$. The matching found using K_W must then link a to b . In contrast, when the edge is excluded, these two elements $[K_W]_{a,b}$ and $[K_W]_{b,a}$ are set to zero, while the others in rows and columns a and b are kept unchanged. If a general matrix A (and hence its inverse A^{-1}) is antisymmetric, numerical stability is enhanced by carrying out both row operations and column operations at the same time, keeping the resulting matrix antisymmetric as well. Using skew-symmetry and applying the Sherman-Morrison formula twice gives the inverse of a matrix modified in two rows and columns as

$$(A + uv^T - (uv^T)^T)^{-1} = A^{-1} - \left(\frac{A^{-1}uv^T A^{-1}}{1 + v^T A^{-1}u} \right) + \left(\frac{A^{-1}uv^T A^{-1}}{1 + v^T A^{-1}u} \right)^T. \quad (19)$$

If an edge e_{ab} is to be removed by setting K_{ab} to zero, then one can set $u_a = 1$ and $v_b = -K_{ij}$, with all other elements of u and v being zero. Similarly, if edge e_{ij} is to be kept, one can also use $u_k = \delta_{a,k}$ for Kronecker delta δ but set the vector v by $v_k = -K_{bk}$, for $\forall k \neq j$.

Given that that matrix A^{-1} is computed directly only once, at the start of spin assignment along a separator, a single update procedure per Eq. 19 may be carried out in $\mathcal{O}(L^2)$ operations for a separator of L spins. This is faster than the $\mathcal{O}(L^3)$ for matrix multiplication of two $L \times L$ matrices because $A^{-1}u$ and $v^T A^{-1}$ are themselves vectors. So performing L updates to the matrix can be achieved in $\mathcal{O}(L^3)$ operations. As the nested dissection produces a separator with $L \propto \sqrt{N}$ elements, sampling across the separator takes $\mathcal{O}(N^{3/2})$ steps. Summing this cost over all of the needed scales for the separators gives a time to sample all of the spins scaling also as $\mathcal{O}(N^{3/2})$.

C. Sampling algorithm outline

Given the connection between K_W^{-1} and spin correlations and the Sherman-Morrison method for updating K_W^{-1} as spins are chosen, the sampling algorithm for periodic systems can now be directly described in outline form:

1. Perform the same up sweep steps needed to compute the cluster matrices U_{A^*} and U_{B^*} . These are the same steps needed to compute the partition function Z but without the final merger.
2. Merge U_{A^*} and U_{B^*} along the line of spins through the middle of the sample that separates the regions A^* and B^* . This is done by placing U_{A^*} and U_{B^*} into a larger matrix and filling in the values of weights w_{ab} along this line. This gives the cluster matrix U_{C^*} which is indexed by nodes along the bottom, top, left, and right rows of the sample.
3. For each of the four global dimer orientations $\pm\pm$, fill in the weights that complete the torus, using signs for the weights given for each choice $(r, s) \in \pm\pm$. This gives four matrices $U_{C^*, \pm\pm}$. Compute the inverse matrices $U_{C^*, \pm\pm}^{-1}$ using Pfaffian elimination (Eq. (9)).
4. For each edge e that connects the top of C^* to the bottom of C^* :
 - (a) Compute the probability that the edge e is occupied using Eq. (17).
 - (b) Apply Eq. (19) to update $U_{C^*, \pm\pm}^{-1}$, using the vectors u and v that modify U_{C^*} so as to force the chosen occupation value of the current edge e .
5. Compute two new cluster matrices, $U_{C_1^*}$ and $U_{C_2^*}$ which have as boundaries the left and right columns of C^* , using the fixed values of the spins in the bottom row chosen in the previous step. Then use a modified form of Eq. (17) that sums only over s , not both r and s , to compute probabilities for edges along the column at the left/right boundary of the sample. After selecting each edge, use Eq. (19) to update $U_{C_1^*}^{-1}$ and $U_{C_2^*}^{-1}$.
6. Use the edge choices, which give portions of relative domain walls, to assign Ising spins around the border of C^* . More specifically, if an edge is chosen to belong to the matching M , the sign of the spin differs on either side of the edge, while if a spin was not chosen, the sign of the two spins on either side is the same.
7. Sampling is now carried out recursively for the subregions, given these fixed boundary conditions around the border of the sample. This is carried out first for the spins lying on the central dividing line between A^* and B^* , and then for the spins lying between their child regions, etc., until all spins are assigned. At each level:
 - (a) Recompute the cluster matrices U_A and U_B for the regions A and B on either side of the separator. This computation uses as a reference configuration all spins $s_i = +1$, except on

the boundary of the region $A \cup B$, where the fixed boundary spins are used as the reference configuration.

- (b) Merge U_A and U_B using the edge weights for edges $e \in W(A, B)$ between A and B to obtain the matrix K_W , the effective Kasteleyn matrix for the separator $W(A, B)$.
- (c) Compute K_W^{-1} by Pfaffian elimination.
- (d) For each of the $|W| - 1$ edges $e \in W$, $e = (i, j)$ for a node i on the boundary of A and a node j on the boundary of B :
 - i. Compute the probability of choosing e , $P(e) = |w_{ij}[K_W^{-1}]_{ij}|$.
 - ii. Choose whether to accept or reject the inclusion of e .
 - iii. Based on whether e is included or excluded from the dimer sampling, set up the vectors u and v and apply the Sherman-Morrison formula to update K_W^{-1} .
- (e) Fix the Ising spins that lie in the separator W using the newly computed portions of the domain walls.

V. APPLICATION AND TIMING

As the implementation of these methods into working programs is relatively complex, we have carried out a number of tests of the code to confirm that it computes partition functions and correlation functions correctly. Previous to this current version of the code, each of the authors has independently written a computer code that computes partition functions using Pfaffians. We confirmed that the two previous codes and the current partition function code [15] compute the same partition function for samples of sizes up to size $L = 256$, for several samples at each size. We have also verified our code by comparison with (1) exact enumeration for small Ising spin glass samples of size up to 5×5 spins and (2) checking correlation functions against analytic results for the ferromagnetic Ising model. The following subsections summarize the results of tests for the pure Ising model and for spin glass models. Similar checks are included as samples in our current distribution of the partition function code [15]. For further examples of applications of these particular codes, see Refs. [10, 11, 26, 27].

A. Verification in small samples

The checks against exact enumeration verified that the code produced both correct partition functions and correlation functions. A simple exact enumeration code computed the Boltzmann factor for each spin configuration S directly, for a given random selection of bond strengths

J_{ij} . The sum of the Boltzmann factors at a given β was compared against the partition function Z computed for each sample using nested dissection and multi-precision arithmetic. In all cases (10^4 random samples for each distribution), the partition functions were in exact agreement. We carried out tests for both bimodal and Gaussian distributions for J_{ij} . As the support for the density of states is limited in the bimodal case when $J_{ij} = \pm 1$, the bimodal distribution allows for an easy exact check of the number of states at each energy. Setting β so that $\exp \beta = 10^m$ for, say, $m = 8$ allows one to directly read off the density of states from Z written in decimal, when the degeneracy at all energies is less than 10^{2m} .

The spin-spin correlations generated by the nested dissection code were also compared with the exact enumeration results and found to be the same. In addition, to check our sampling code, up to 10^6 configurations were generated using our sampling methods for several $L = 5$ samples. The temperatures used were set so that about 90% of the configurations were in one of the ten lowest energy states. The temperature was set this low to have enough statistics to verify the Boltzmann distribution for the low-lying states, including the degeneracies of the bimodal distribution. The distribution of energies found were also found to satisfy the Boltzmann distribution for Gaussian disorder, where there is a unique state for each energy.

B. Verification of correlations using the ferromagnetic model

To check the calculation directly against an analytic result in larger samples, we numerically computed the spin-spin correlation function for the square lattice in ferromagnetic Ising models at the critical temperature. For $J_{ij} = 1$ for all neighboring pairs on the square the lattice, the critical temperature T_c satisfies $T_c^{-1} = \beta_c = \frac{1}{2} \ln(\sqrt{2} + 1)$ for $J_{ij} = 1$. The correlation function along the diagonals, $\langle s_{0,0} s_{n,n} \rangle$, where the spins are now indicated by two subscripts that indicate their x and y coordinates on the lattice. The computed correlation function was compared with known results [28, 29]. While this does not check for the effect of heterogeneities on correlation functions, it helps confirm that correlation calculations are carried out correctly at all scales, from single sites up through the size of the sample. The analytic result [29] for an infinite sample is

$$\langle s_{0,0} s_{R,R} \rangle = \left(\frac{2}{\pi}\right)^R \prod_{i=1}^{R-1} \left[1 - \frac{1}{4i^2}\right]^{i-R} \quad (20)$$

Z which at large separations $|i - j| = R\sqrt{2} \gg 1$ gives

$$\langle s_{0,0} s_{R,R} \rangle = a_0 |i - j|^{-1/4}, \quad (21)$$

with $a_0 = 2^{1/12} e^{3\zeta'(-1)}$ and ζ is the Riemann ζ function. The numerical results for finite-size samples are plotted

in Fig. 8. The rather large finite-size corrections to the spin-spin correlation functions are apparent, but the numerical calculation quickly converges to the exact short distance results of Eq. (20) and apparently converges to the asymptotic limit Eq. (21), giving us further confidence in the correlation function code.

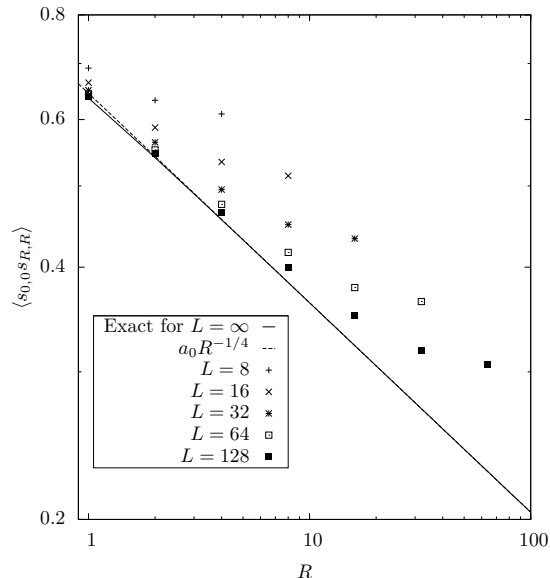


Figure 8: Plot of correlation functions for the ferromagnetic Ising model at criticality. The correlation function $\langle s(0,0)s(R,R) \rangle$ for diagonal spin separations (R,R) was computed using Pfaffian methods for samples of size $L \times L$ spins, $L = 8, \dots, 128$, and compared with $L = \infty$ exact and asymptotic results.

C. Timings

We conclude the review of these algorithms with a list of the timings and memory used, in order to compare with other implementations and algorithms. Table I gives average run times on a single core of a 2.4 GHz Xeon E5620 quad-core processor with 12 GB of memory. The GNU multiprecision arithmetic library `gmp` (version 3.5.0) was utilized for high precision floating point arithmetic using the C++ interface `gmpxx` (version 4.1.0) included with `gmp` [30]. Multiprecision arithmetic was used for all floating point calculations, including the temperature parameters, storing the bond strengths and weights, and all matrix and partial Pfaffian operations. A pair

of custom routines were written for the logarithm and exponential functions. These are used only for computing weights at the start of the computation and computing logarithms of the partition functions at the end of the calculation, for finding free energies. These timings are all for periodic samples: for samples with free or fixed boundary conditions, approximately four times less memory and CPU time are needed. As long as there are no overflows, the running time is independent of inverse temperature β , though increasing the precision increases the maximum value of β for which the calculations are stable. For $L = 256$ and bimodal disorder, floats using 1536 bits are needed to reliably sample configurations for $\beta = 20$. Computing the partition function or using Gaussian disorder requires just somewhat fewer bits.

VI. FUTURE WORK

The goal of this paper has been to present in detail numerical methods for computing thermodynamic quantities, computing spin-spin correlation functions, and sampling configurations for two-dimensional Ising models with short range (planar) interactions. The development and explication of these methods, which incorporates many ideas from previous work, emphasizes the natural summing over various length scales. Especially at lower temperatures, the near cancellations that result during the matrix operations require matrix operations with multi-precision arithmetic. The precise numerical results obtained are a great advantage for studying thermodynamic quantities, compared with traditional Markov Chain Monte Carlo methods, for a broad range of problems. We have prepared a code that should be easily compiled to compute partition functions for the Ising model with arbitrary couplings on square lattices. We are currently preparing implementations of the correlation function and sampling codes for distribution. The structure of the algorithm is also very suggestive with respect to the renormalization of couplings in random models, which might be studied directly to look for some type of fixed point distribution in coarse grained couplings.

We thank Cris Cecka for introducing us to the FIND algorithm of Ref. [14]. This work was supported in part by the National Science Foundation grant DMR-1006731. We thank the Aspen Center for Physics, supported by NSF grant 1066293, for its hospitality while portions of this paper were written up.

-
- [1] P. W. Kasteleyn, *Physica* **27**, 1209 (1961).
 - [2] H. N. V. Temperley and M. E. Fisher, *Phil. Mag.* **6**, 1061 (1961); M. E. Fisher, *Phys. Rev.* **124**, 1664 (1961).
 - [3] P. W. Kasteleyn, *J. Math. Phys.* **4**, 287 (1963).
 - [4] M. E. Fisher, *J. Math. Phys.* **7**, 1776 (1966).

- [5] H. S. Robertson, “Statistical Thermophysics” (Prentice Hall, 1993).
- [6] W. Krauth, “Statistical Mechanics: Algorithms and Computations” (Oxford University Press, 2006).
- [7] L. Saul and M. Kardar, *Phys. Rev. E* **48** R3221 (1993).

System size	Floating point precision (bits)	CPU time, compute Z	Peak memory, compute Z	CPU time, correlations	Peak memory, correlations	CPU time, choose configuration	Peak memory, choose configuration
16	128	0.21 s		3.0 s		0.47 s	
16	512	0.45 s		3.9 s		0.83 s	
16	2048	2.9 s				4.75 s	5.1 MB
32	128	1.0 s		18 s	13 MB	3.7 s	4.9 MB
32	512	2.2 s		33 s	17 MB	6.3 s	6.8 MB
32	2048	15 s	11 MB			37.1 s	37 MB
64	128	5.9 s	10 MB	173 s	47 MB	29.0 s	15 MB
64	512	13 s	15 MB	311 s	67 MB	50.4 s	45 MB
64	2048	85 s	38 MB			301 s	78 MB
128	128	40 s	35 MB	1873 s	200 MB	—	—
128	512	82 s	57 MB	2888 s	281 MB	348 s	87 MB
128	2048	552 s	146 MB			2454 s	222 MB
256	128	304s	135 MB			—	—
256	512	605 s	224 MB			3418 s	240 MB
256	2048	3946 s	580 MB			20268 s	899 MB

Table I: A listing of timings and peak memory used by the Pfaffian nested dissection algorithms for different calculations. The resource usage shown is for the computation for a single sample defined by bond strengths J_{ij} . Timings and memory usage are displayed for computing partition functions Z , for computing correlation functions between all spins at the corners of the geometric dissection, and for choosing a single configuration sampled exactly from the Boltzmann distribution. The results are listed as a function of the size of the square sample, with $N = L^2$ spins, and the floating point precision used. See the text for a brief description of the hardware and multi-precision arithmetic libraries that were used. Blank entries in this table indicate where measurements were not made; dashes indicate where the matrix inverse used in the sampling method was unstable.

- [8] A. Galluccio, M. Loebl, and J. Vondrak, Phys. Rev. Lett. **84**, 5924 (2000).
- [9] T. Jörg, J. Lukic, E. Marinari, and O. C. Martin, Phys. Rev. Lett. **96**, 237205 (2006).
- [10] C. K. Thomas, D. H. Huse, and A. A. Middleton, Phys. Rev. Lett. **107**, 047203 (2011).
- [11] C. K. Thomas and A. A. Middleton, Phys. Rev. E **80**, 046708 (2009).
- [12] D. B. Wilson, Proceedings of the Eighth Symposium on Discrete Algorithms (SIAM, Philadelphia, 1997) p. 258.
- [13] J. Poulter and J. A. Blackman, Phys. Rev. B **72** 104422 (2005).
- [14] S. Li, S. Ahmed, G. Klimeck and E. Darve, J. Comp. Phys. **227**, 9408 (2008).
- [15] See <http://physics.syr.edu/~aam/software> for source code.
- [16] F. Barahona, J. Phys. A **15** 3241 (1982).
- [17] C. K. Thomas and A. A. Middleton, Phys. Rev. B **76**, 220406(R) (2007).
- [18] M. Kac and J. C. Ward, Phys. Rev. **88**, 1332 (1952).
- [19] This cancellation can most directly be understood in terms of Fisher cities. The Fisher mapping from the Ising model to a dimer model is one-to-one, and if one performs Pfaffian elimination on the two inner nodes of a Fisher city, a Kasteleyn city results. The two different types of decorations are equivalent, forcing this convenient cancellation.
- [20] R. J. Lipton, D. J. Rose, and R. E. Tarjan, SIAM (Soc. Ind. Appl. Math.) J. Numer. Anal. **16**, 346 (1979).
- [21] James R. Bunch, Math. Comp. **38**, 475 (1982).
- [22] M. E. J. Newman and G. T. Barkema, “Monte Carlo Methods in Statistical Physics” (Clarendon Press, Oxford, 1999).
- [23] J. G. Propp and D. B. Wilson, Random Struct. Algorithms **9**, 223 (1996).
- [24] C. Chanal and W. Krauth, Phys. Rev. Lett. **100**, 060601 (2008).
- [25] R.A. Martin and D. Randall (1999). 3rd International Workshop on Randomization and Approximation Techniques in Computer Science in Lecture Notes in Computer Science, 1671: 257-268.
- [26] C. K. Thomas, D. A. Huse, A. A. Middleton, <http://arxiv.org/cond-mat/1012.3444>.
- [27] C. K. Thomas and H. G. Katzgraber, Phys. Rev. E **84**, 040101(R) (2011).
- [28] E. W. Montroll, R. B. Potts and J. C. Ward, J. Math. Phys. **4**, 308 (1963).
- [29] H. Cheng and T. T. Wu, Phys. Rev. **164**, 719 (1967).
- [30] See the software releases and the manual by T. Granlund at <http://gmplib.org>.